

Pitfalls in using statistical bias-correction methods to characterize climate change impacts

Nicolás A. Vásquez¹, Pablo A. Mendoza^{1,2}, Wouter J. M. Knoben³ *, Louise

Arnal³ †, Miguel Lagos-Zúñiga⁴, Martyn Clark³ ‡, Ximena Vargas¹

¹Department of Civil Engineering, Universidad de Chile

²Advanced Mining Technology Center, Universidad de Chile

³Centre for Hydrology, University of Saskatchewan, Canmore, Alberta, Canada

⁴Center for Climate and Resilience Research, Universidad de Chile

Corresponding author: N. A. Vásquez, Department of Civil Engineering, Universidad de Chile,
2002 Almirante Blanco Encalada Av., Santiago, 8370449, Chile. (nicolas.vasquez.pl@uchile.cl)

*Department of Civil Engineering,
Schulich School of Engineering, University
of Calgary, Calgary, Alberta, Canada

†now at Ouranos, Montreal, Quebec,
Canada

‡Department of Civil Engineering,
Schulich School of Engineering, University
of Calgary, Calgary, Alberta, Canada

Contents of this file

1. Figures S1 to S19 expand the results to other climate indices since the main manuscript only contains results for precipitation at different time scales.

Additional Supporting Information (Files uploaded separately)

1. Taylor Skill Score (Taylor, 2001) for (i) each climate region (ds01) and (ii) grid cell (ds02), uploaded as excel (.xlsx) files.
2. Grid cells' coordinates and attributes used for clustering (ds03; as .csv).

Introduction. The material included here expands the results presented for precipitation (during the historical period) to the rest of the climate indices: (i) air temperature (T), (ii) diurnal temperature range (DTR), (iii) precipitation (P), (iv) coefficient of variation of inter-annual precipitation (c.o.v. P), (v) 1% highest daily precipitation (P-1%), (vi) wet spell length (WSL), (vii) dry spell length (DSL), (viii) wet fraction (WF) and (ix) snowfall fraction (SF). Figures S1 to S9 display the biases at the annual, seasonal, and monthly time scales. Figures S10 to S19 show the results of the Analysis of Variance (ANOVA). Two additional files were uploaded separately. They contain the Taylor Skill score values (TSS) for each grid cell and also the TSS computed at the climate cluster scale. TSS cluster values were calculated from the mean cluster precipitation seasonality for the period 1980-2014 (as the grid cell average within each cluster).

Biases After Applying Correction Methods Figures S1 to S9 display the bias of each climate index at the annual and monthly time scales, disaggregated by the temporal stratification (TS) considered to bias correct the raw GCM outputs (entire period, seasons, and months). When not shown, the unit of the bias corresponds to the difference between the bias-corrected GCM and the reference ($X_{GCM} - X_{ref}$).

Relative Importance to Remove Biases. Figure S10 shows the relative importance of the bias correction method (BCM) and the TS to explain the variance of errors in bias-corrected climate indices during the historical period for Continental Chile, based on Analysis of Variance (ANOVA). The Total Variance (TV) is formulated as $TV = BCM + TS + Residuals$. Results from the ANOVA analysis (BCM/TV , TS/TV , and $Residuals/TV$) are computed for each grid cell and GCM and subsequently averaged for continental Chile. Figures S11 to S19 show the same results, disaggregated by climate clusters.

References

- Taylor, K. E. (2001, 4). Summarizing multiple aspects of model performance in a single diagram. *Journal of Geophysical Research: Atmospheres*, 106(D7), 7183–7192. doi: 10.1029/2000JD900719

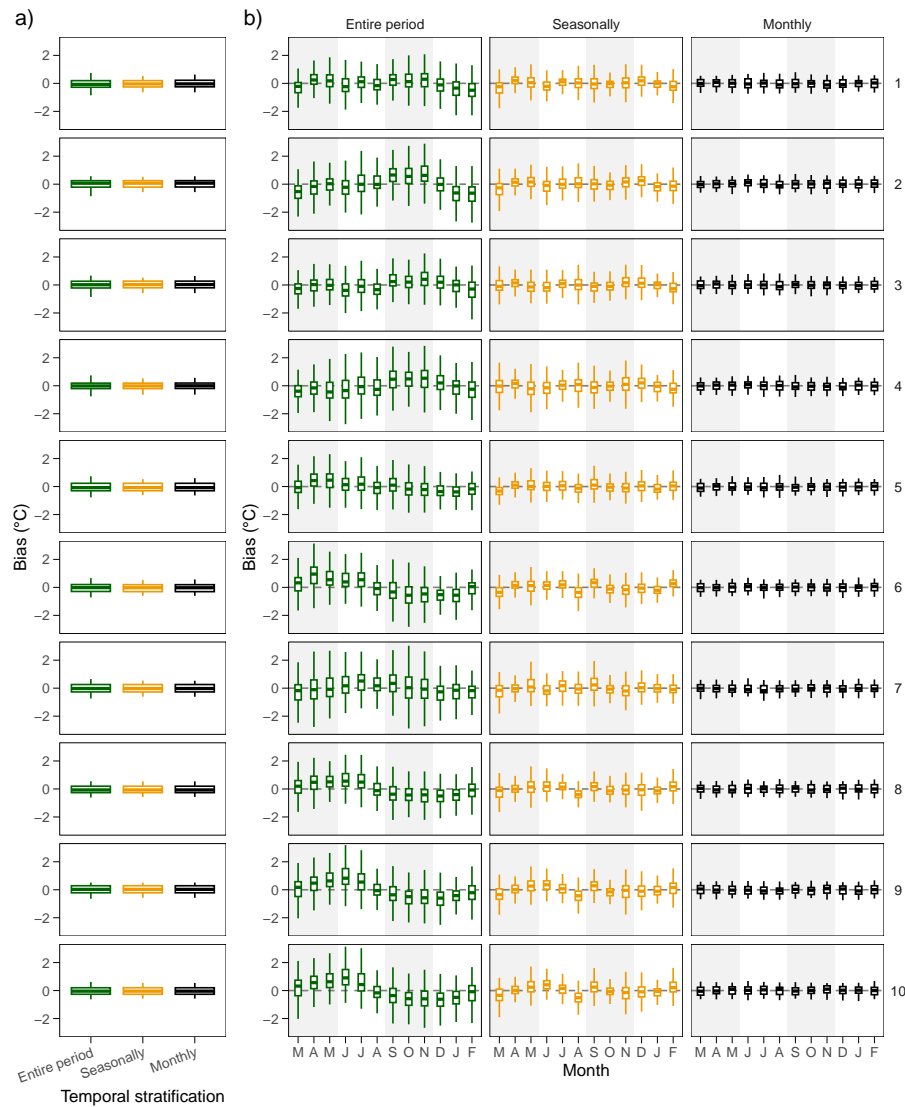


Figure S1. Temperature bias at the (a) annual and (b) monthly time scales after bias correction, separated for each climatic group (rows). The colors indicate the temporal stratification used to apply the BCM. Biases are computed for the 1980-2014 period.

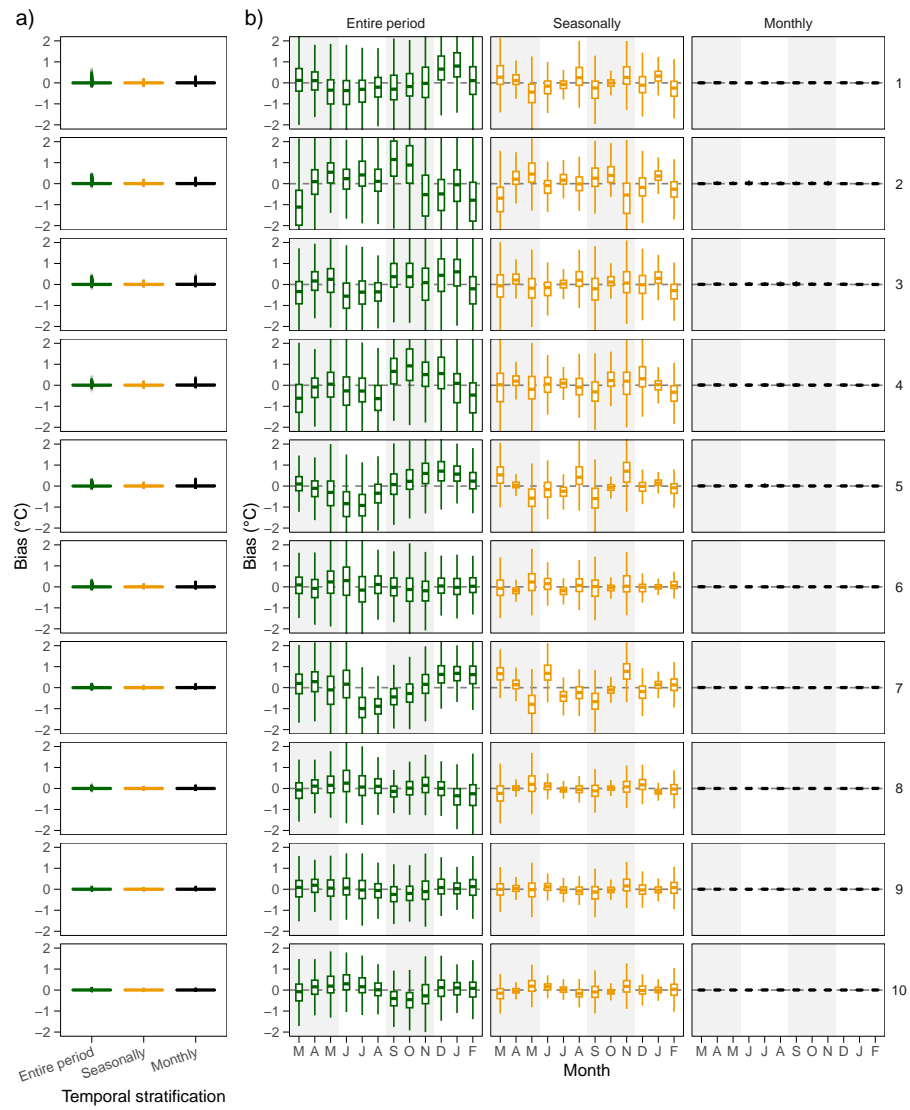


Figure S2. Same as Figure S1, but for diurnal temperature range.

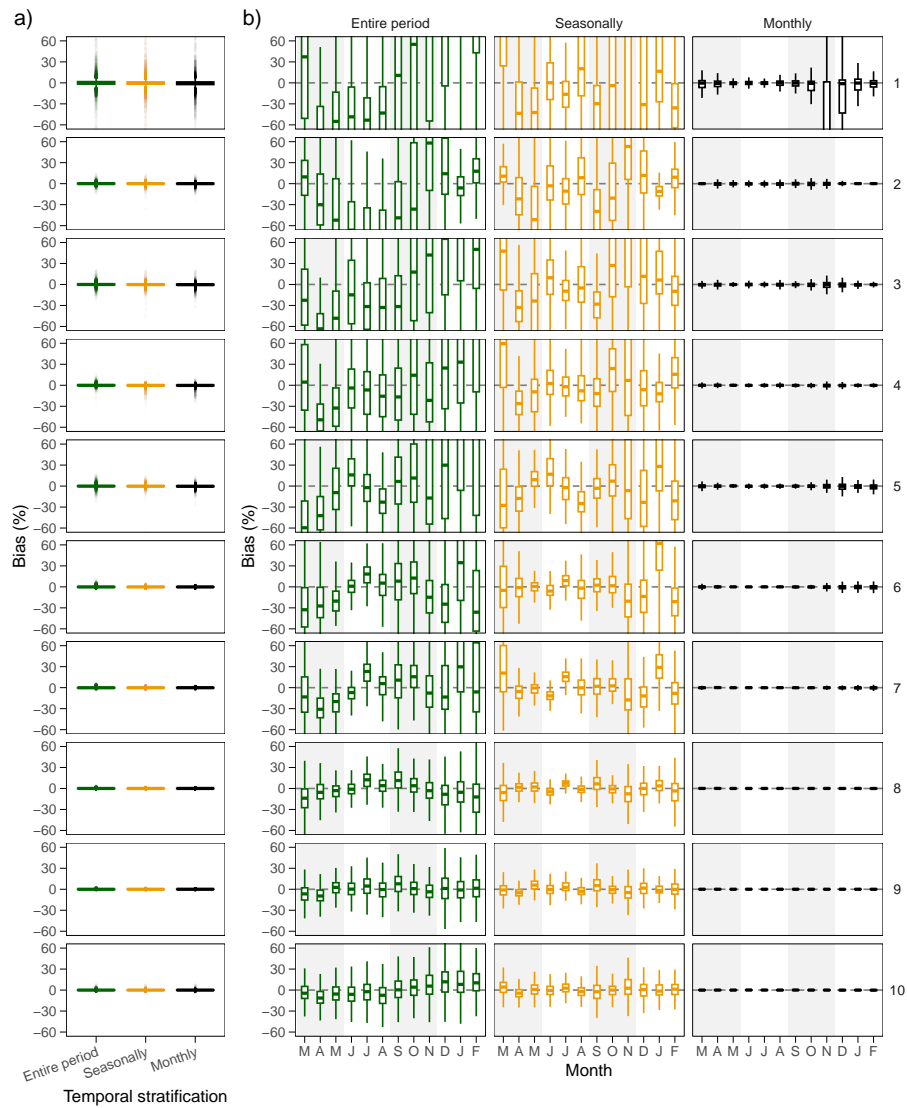


Figure S3. Same as in Figure S1, but for precipitation

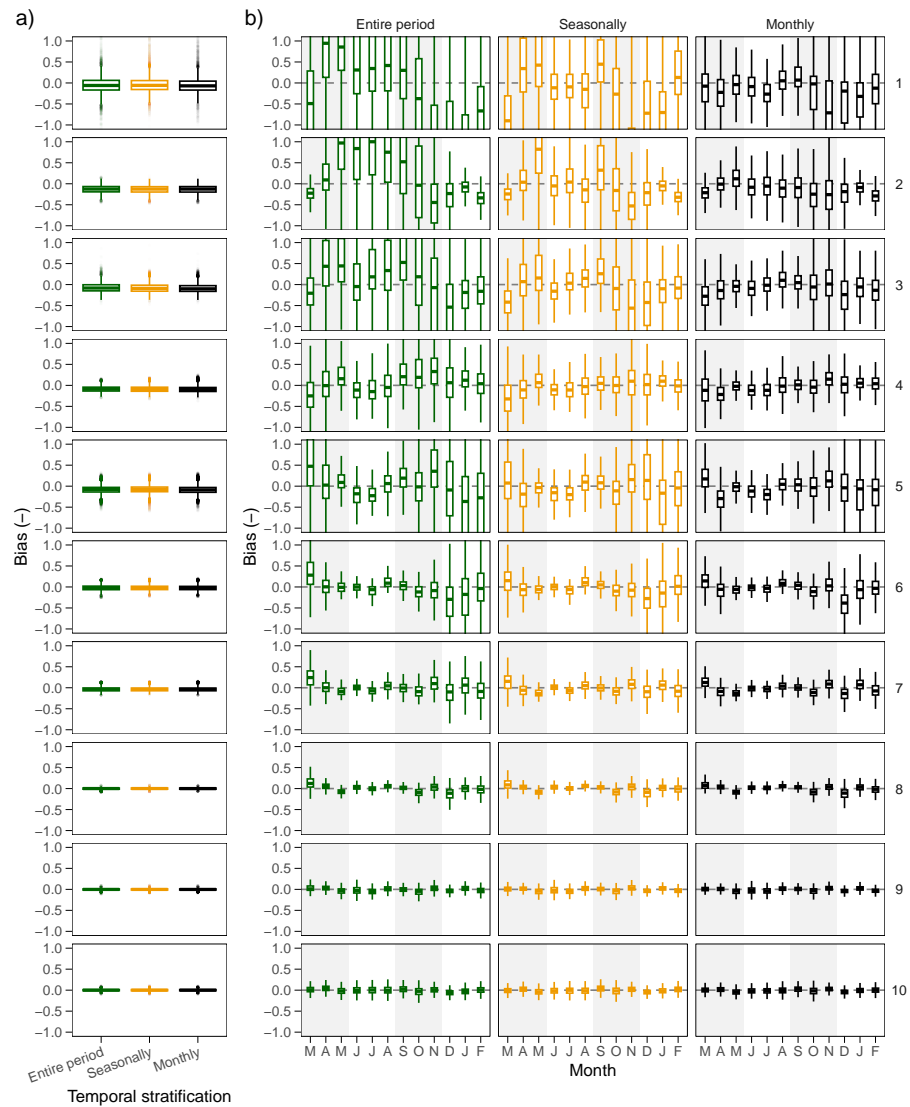


Figure S4. Same as Figure S1, but for the coefficient of variation for inter-annual precipitation

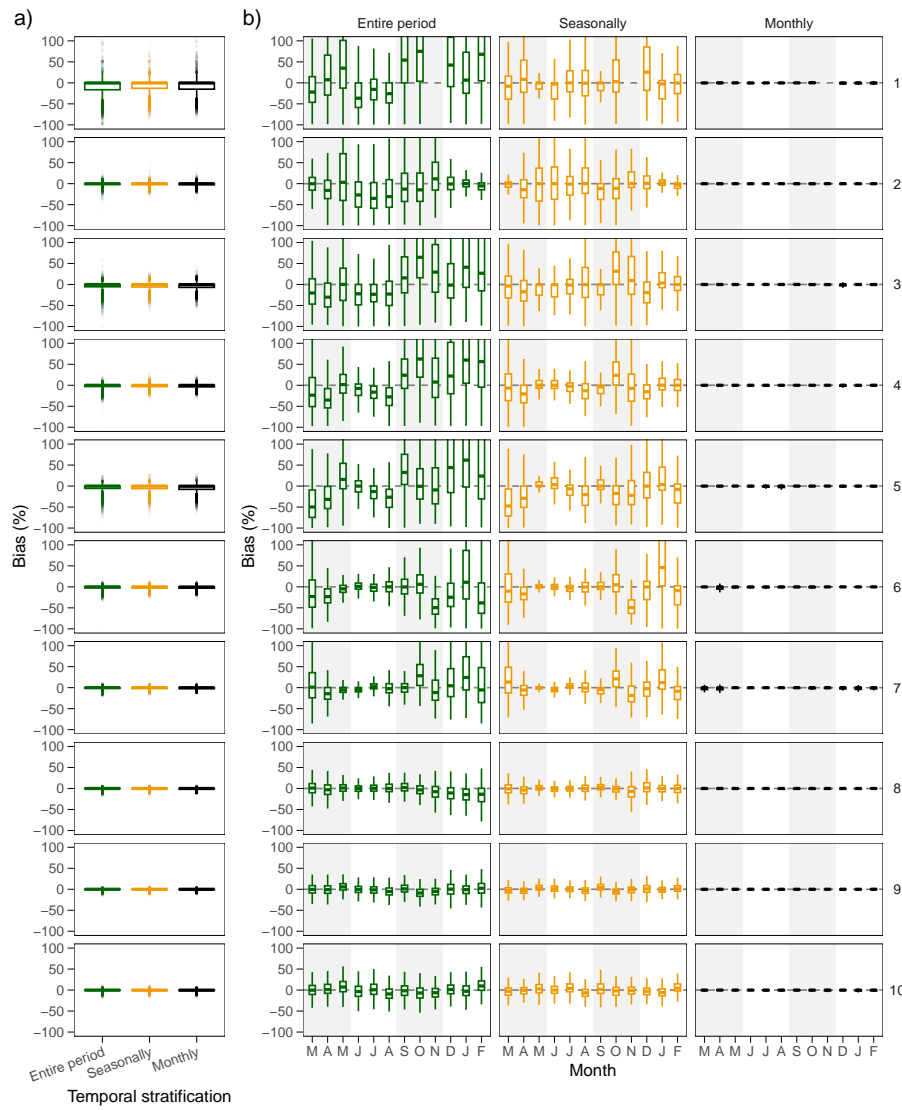


Figure S5. Same as in Figure S1, but for the highest 1% daily precipitation

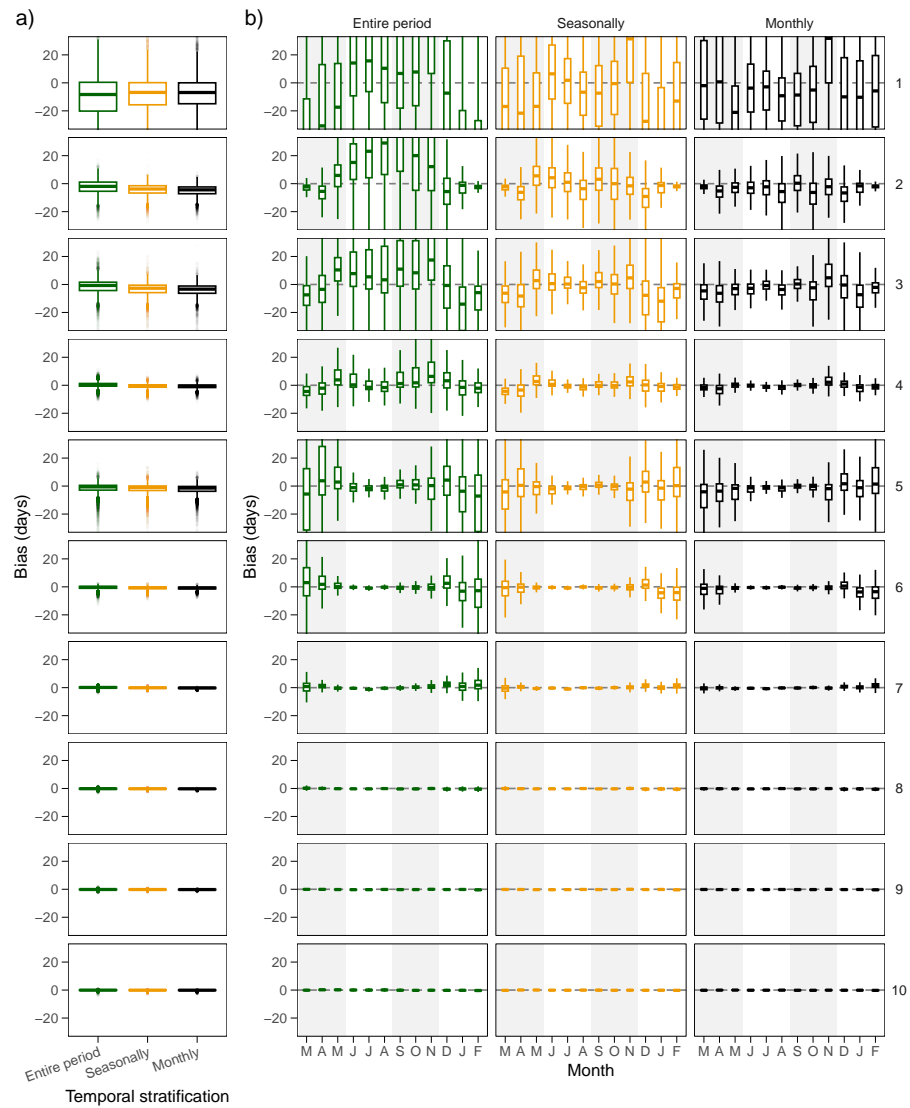


Figure S6. Same as in Figure S1, but for the dry spell length

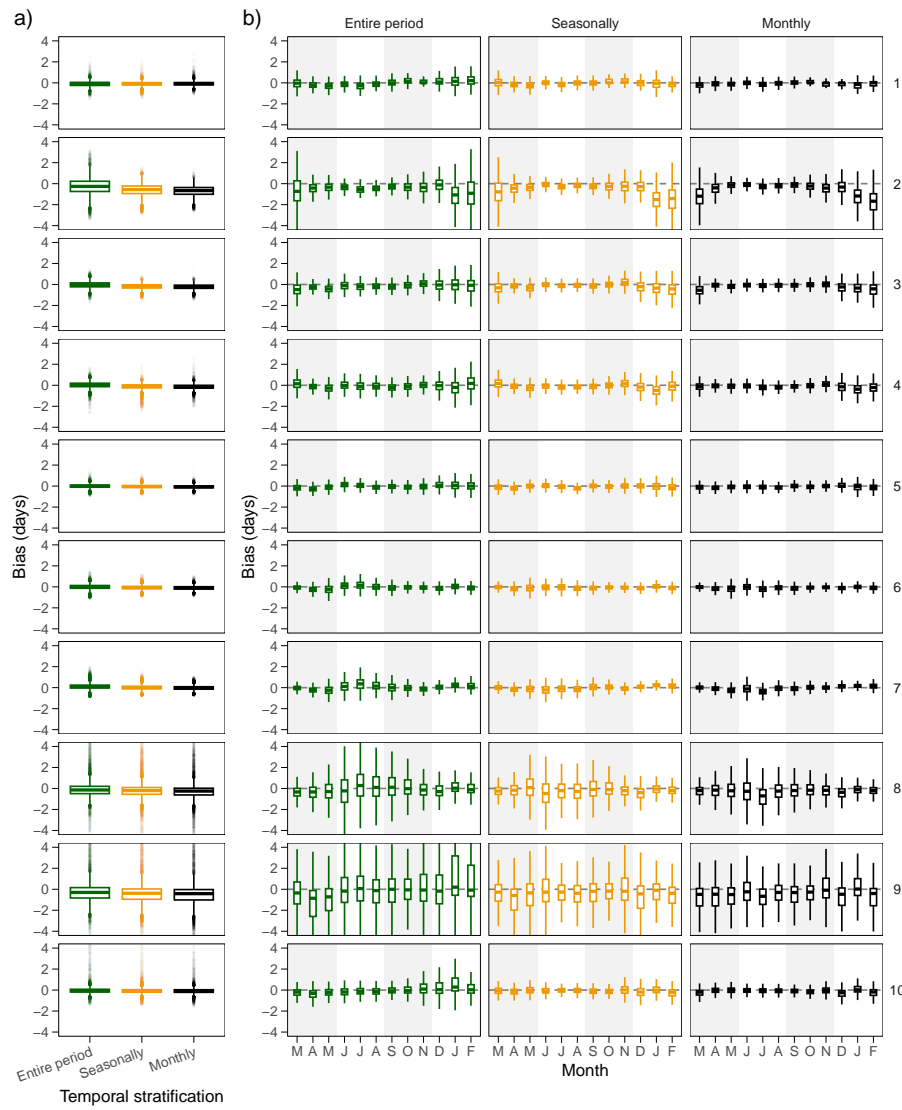


Figure S7. Same as in Figure S1, but for the wet spell length

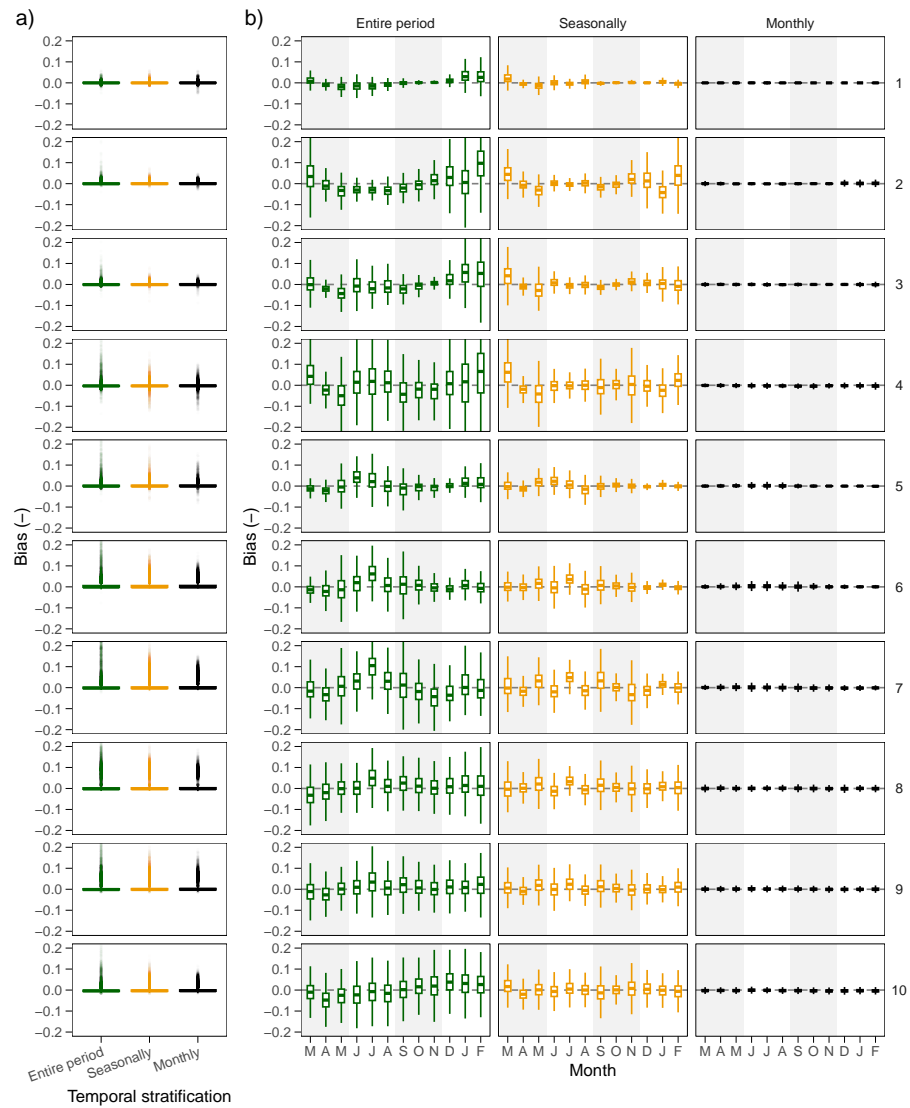


Figure S8. Same as in Figure S1, but for the wet day fraction

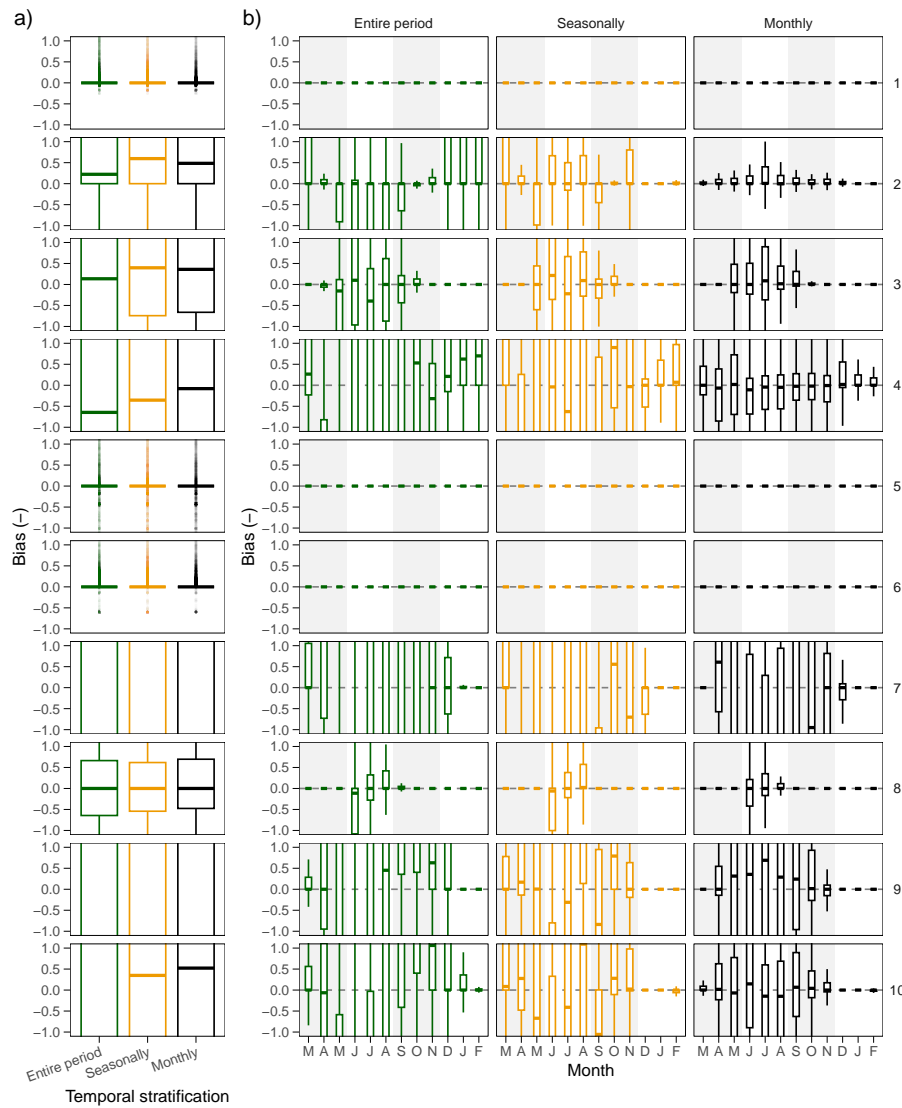


Figure S9. Same as in Figure S1, but for the snowfall fraction

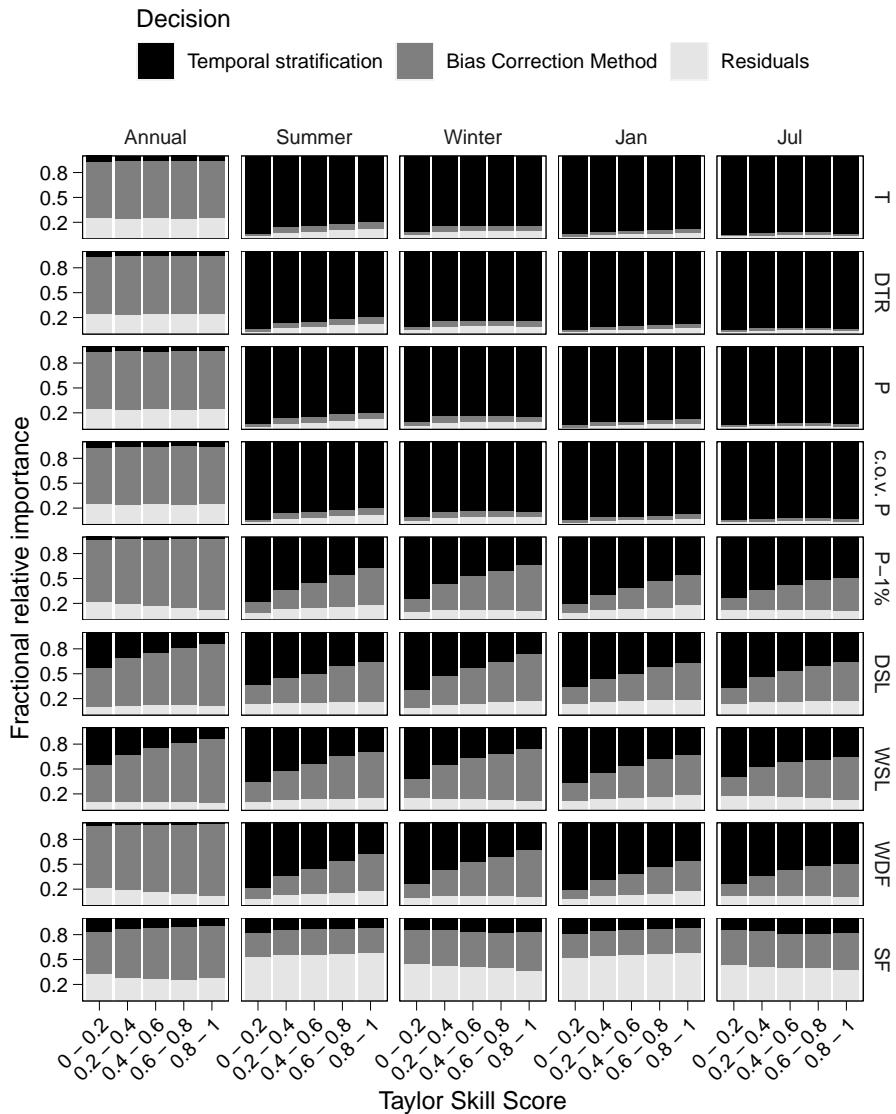


Figure S10. Relative importance (averaged across all grid cells and GCMs) of the bias correction method and the temporal stratification to explain the dispersion of biases with respect to the reference dataset at the annual, seasonal (DJF and JJA), and monthly (January and July) time scales during the historical period (1980-2014). Results are stratified according to the historical raw GCM performance (measured by the TSS; x-axis). Biases are computed after applying the BCMs, and results are displayed for temperature (T), diurnal temperature range (DTR), precipitation (P), coefficient of variation of inter-annual precipitation (c.o.v. P), highest 1% daily precipitation amount (P-1%), dry spell length (DSL), wet spell length (WSL) and snowfall fraction (SF).

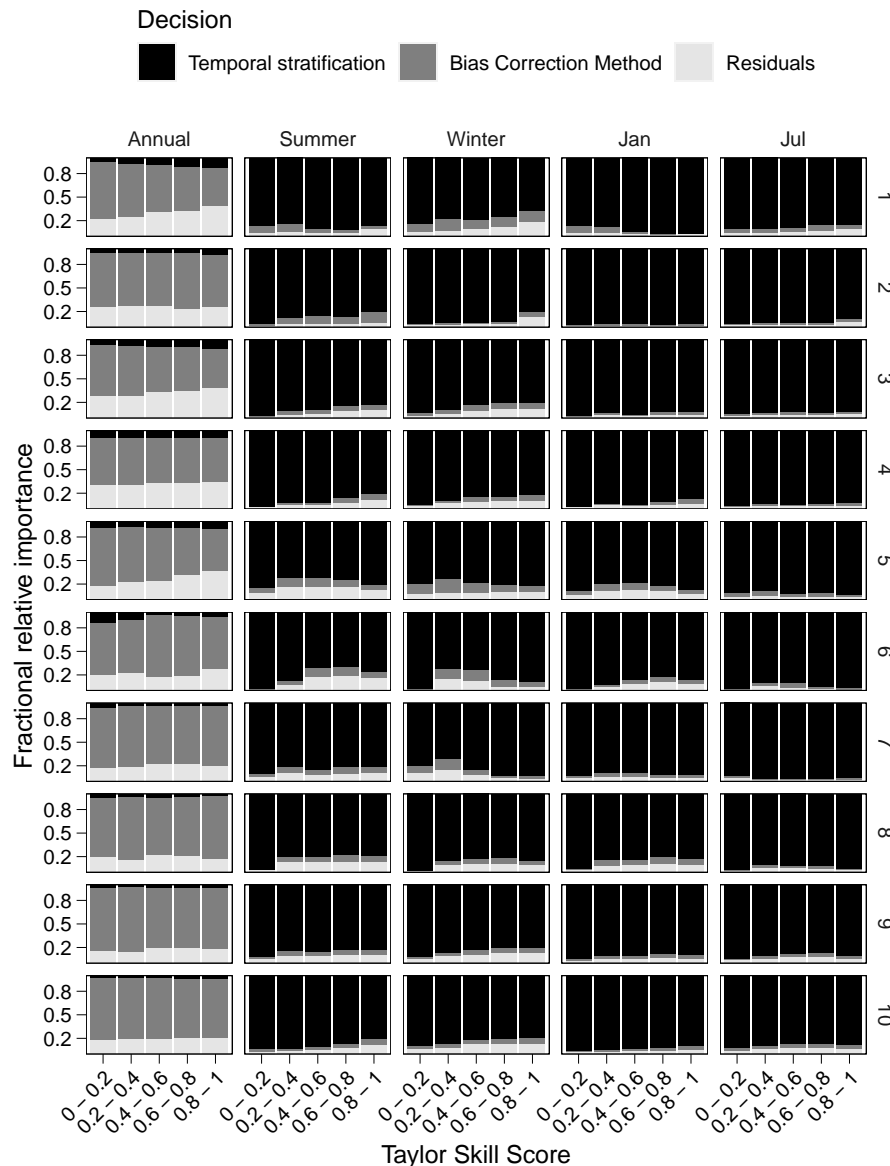


Figure S11. Relative importance (averaged across all GCMs and grid cells within each climate group) of the bias correction method and the temporal stratification to explain the dispersion of temperature biases (with respect to the reference dataset) at the annual, seasonal (DJF and JJA), and monthly (January and July) time scales during the historical period (1980-2014). Results are stratified according to the historical raw GCM performance (measured by the TSS; x-axis) and climate group (rows). Biases are computed after applying the BCMs.

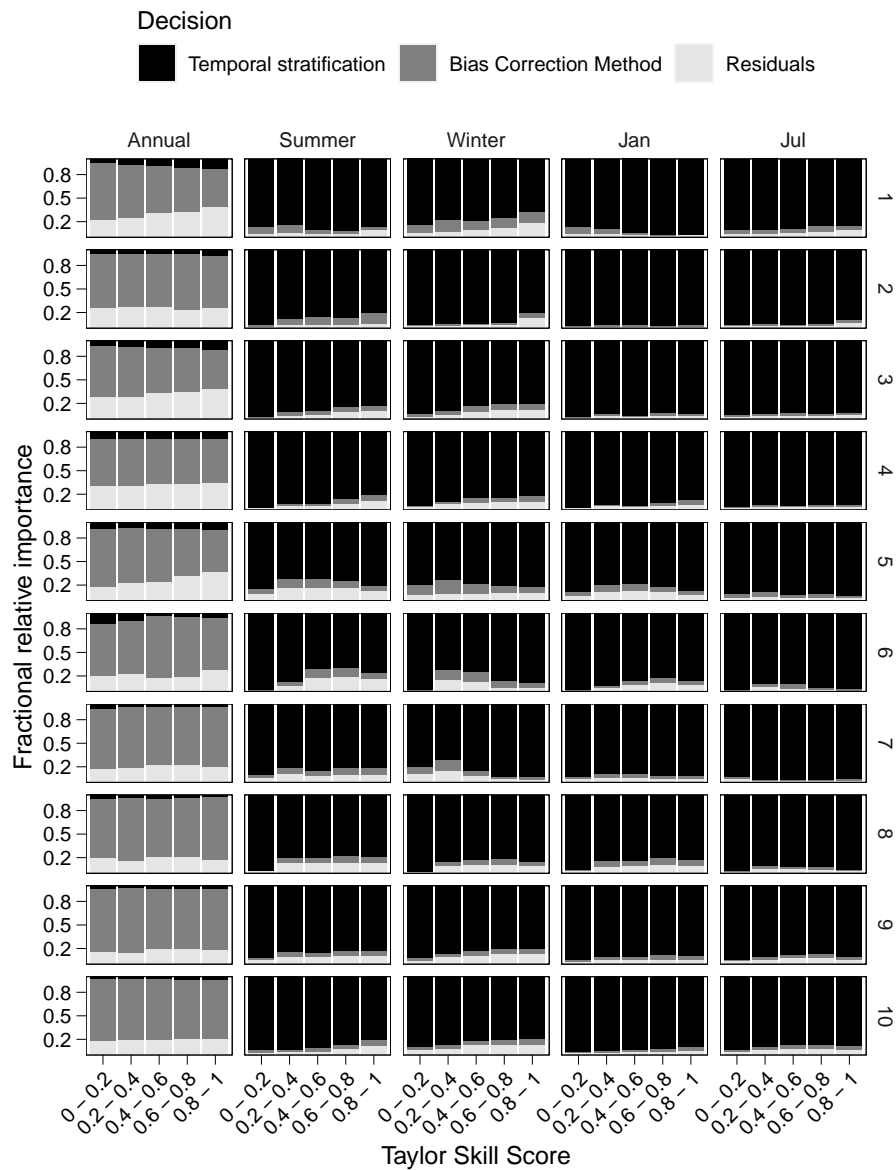


Figure S12. Same as in Figure S11, but for diurnal temperature range.

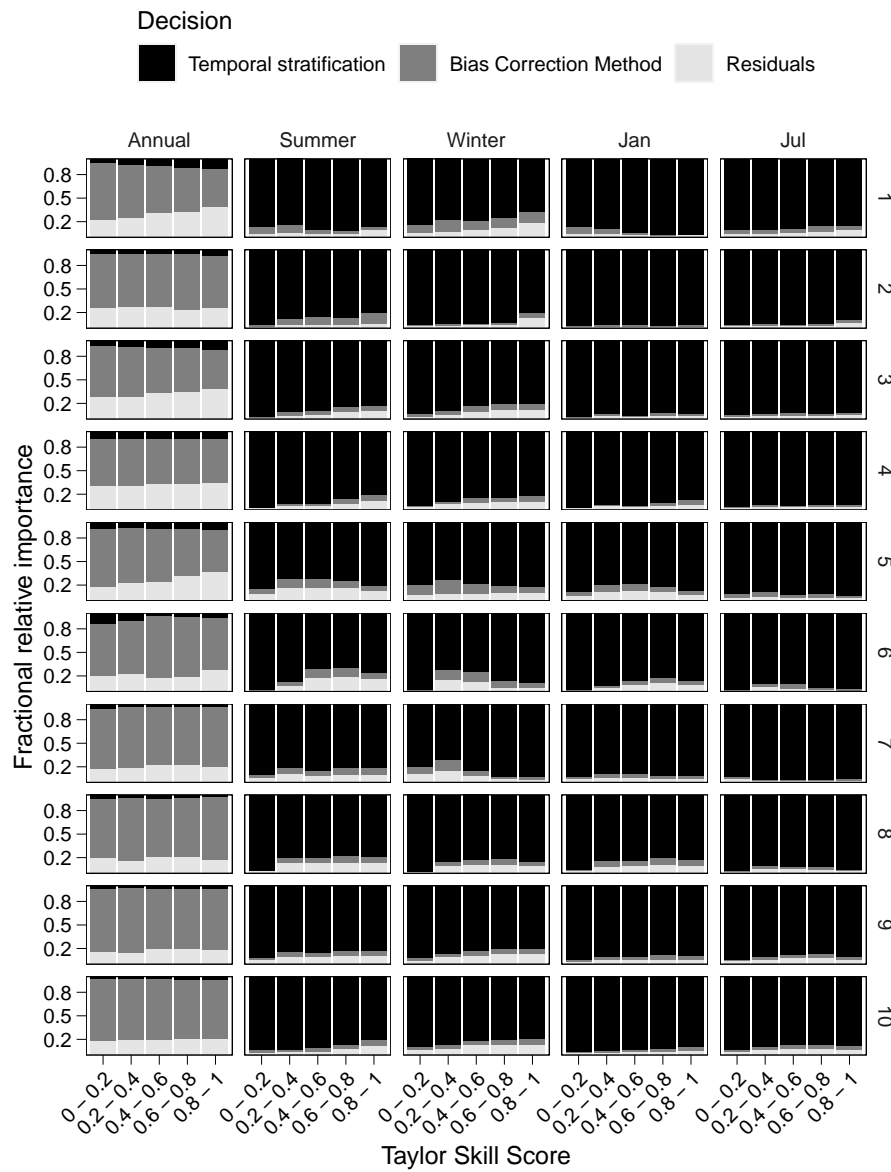


Figure S13. Same as in Figure S11, but for precipitation.

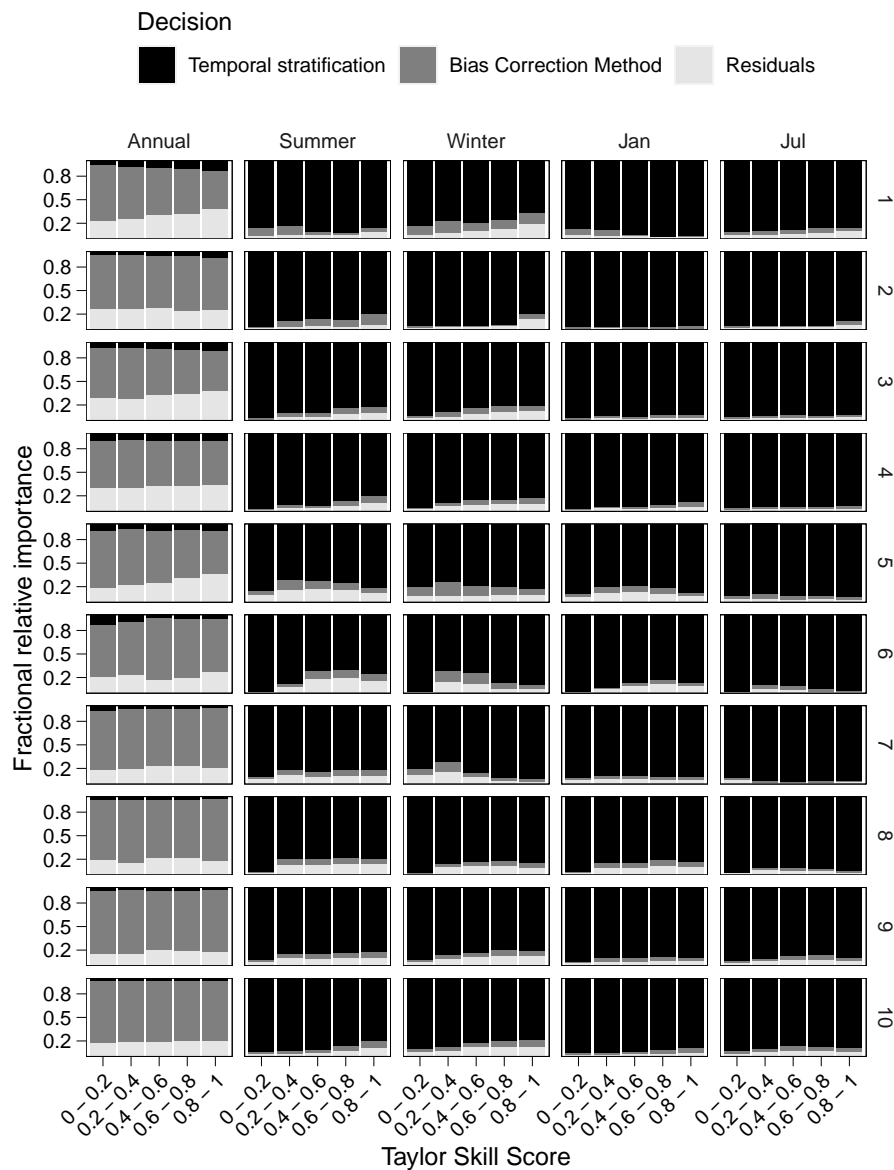


Figure S14. Same as in Figure S11, but for the coefficient of variation of inter-annual precipitation.

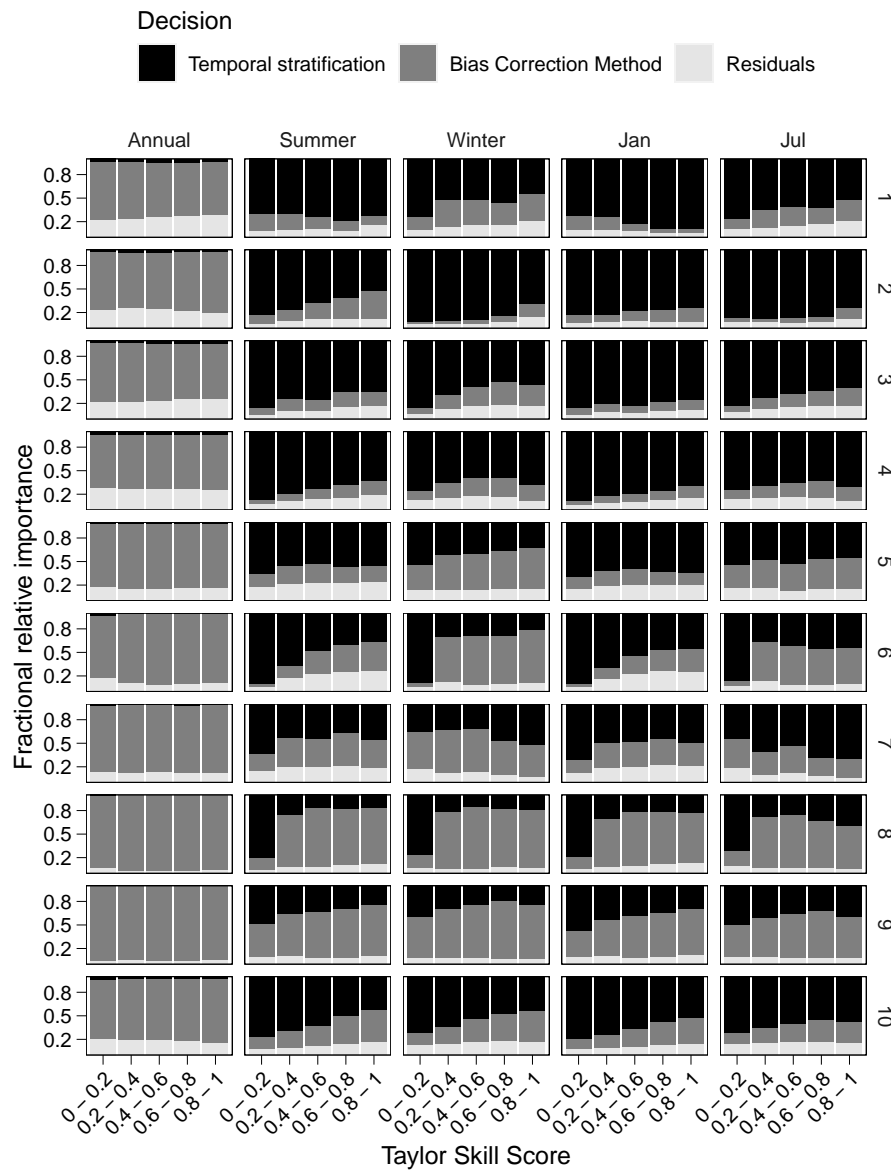


Figure S15. Same as in Figure S11, but for the highest 1% daily precipitation.

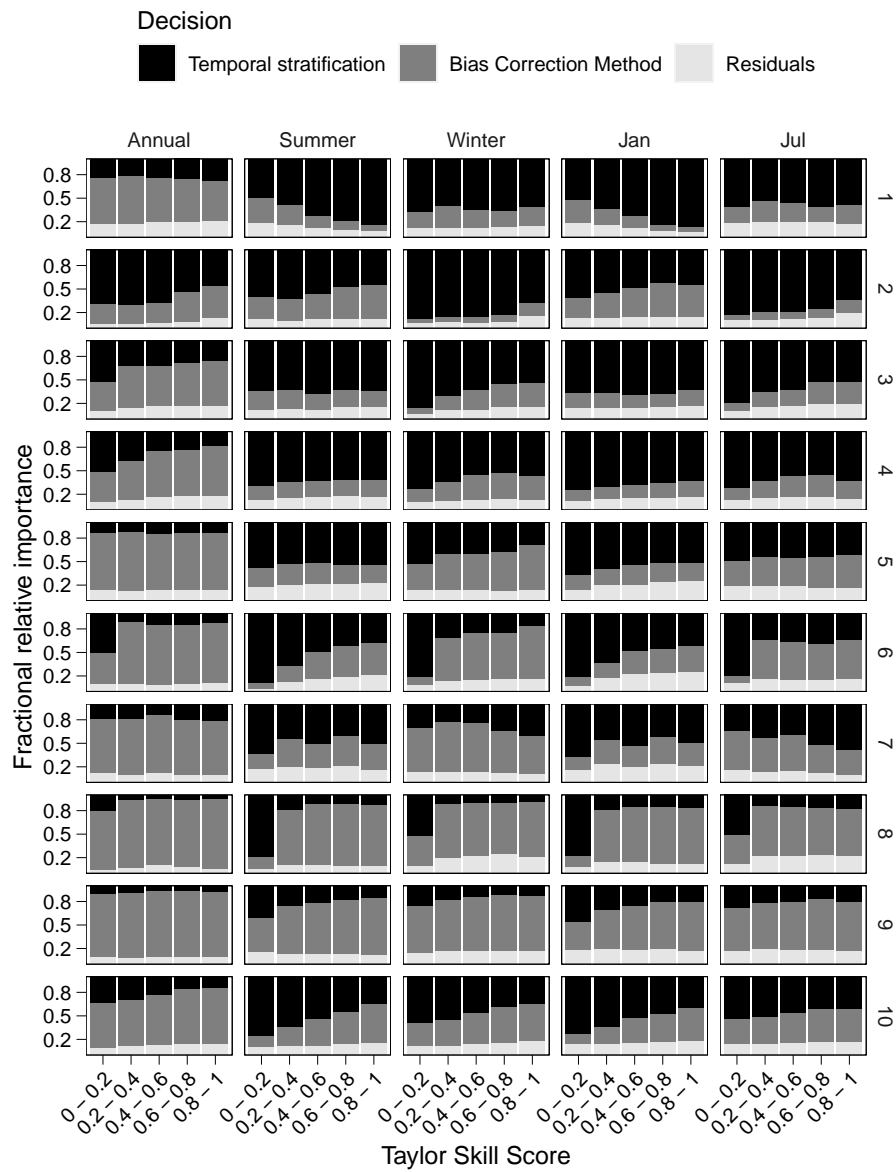


Figure S16. Same as in Figure S11, but for dry spell length.

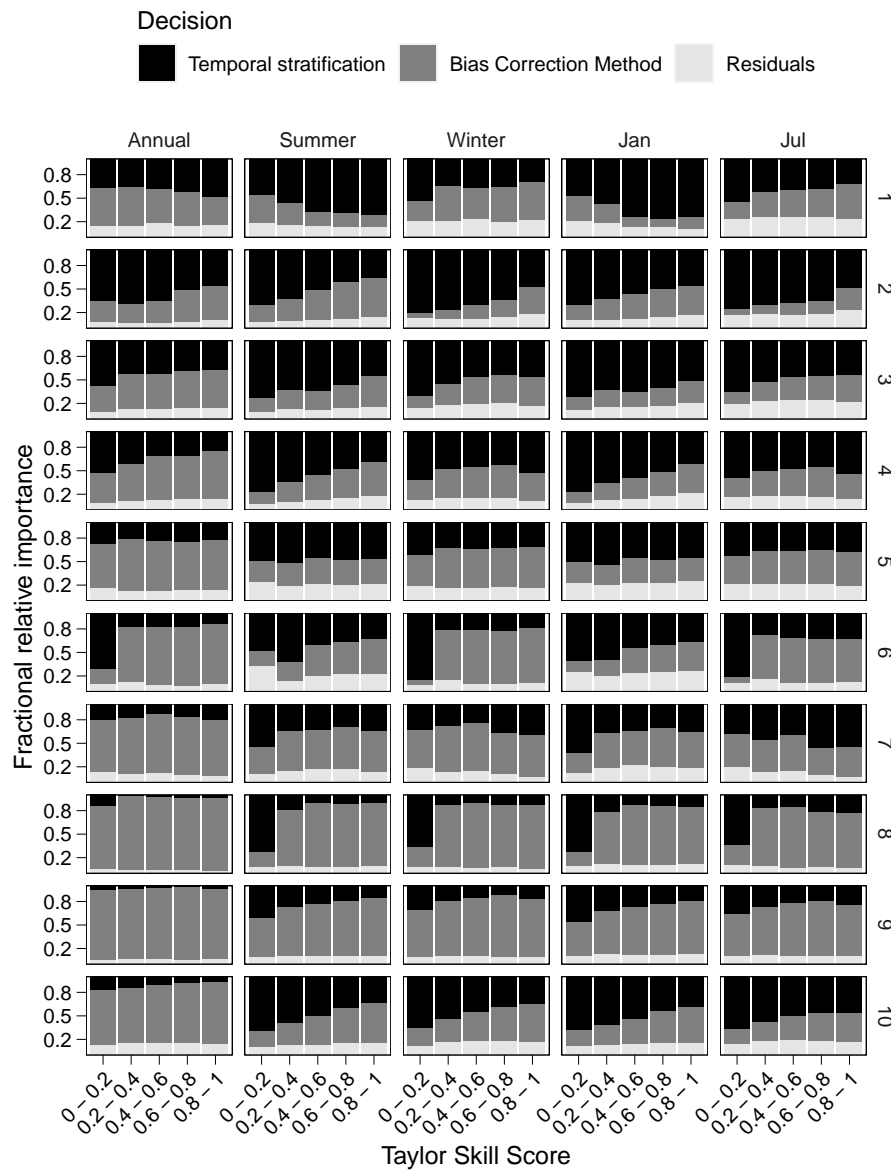


Figure S17. Same as in Figure S11, but for wet spell length.

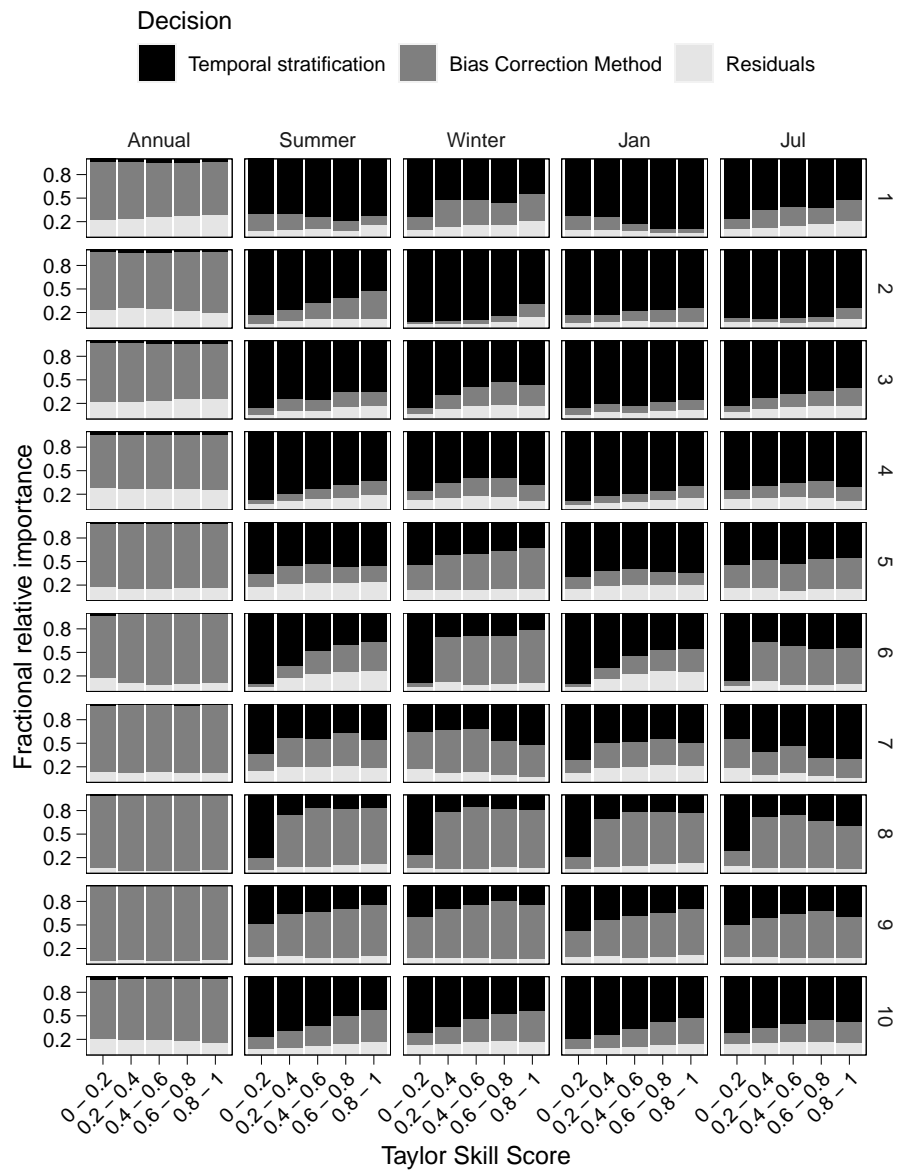


Figure S18. Same as in Figure S11, but for wet day fraction

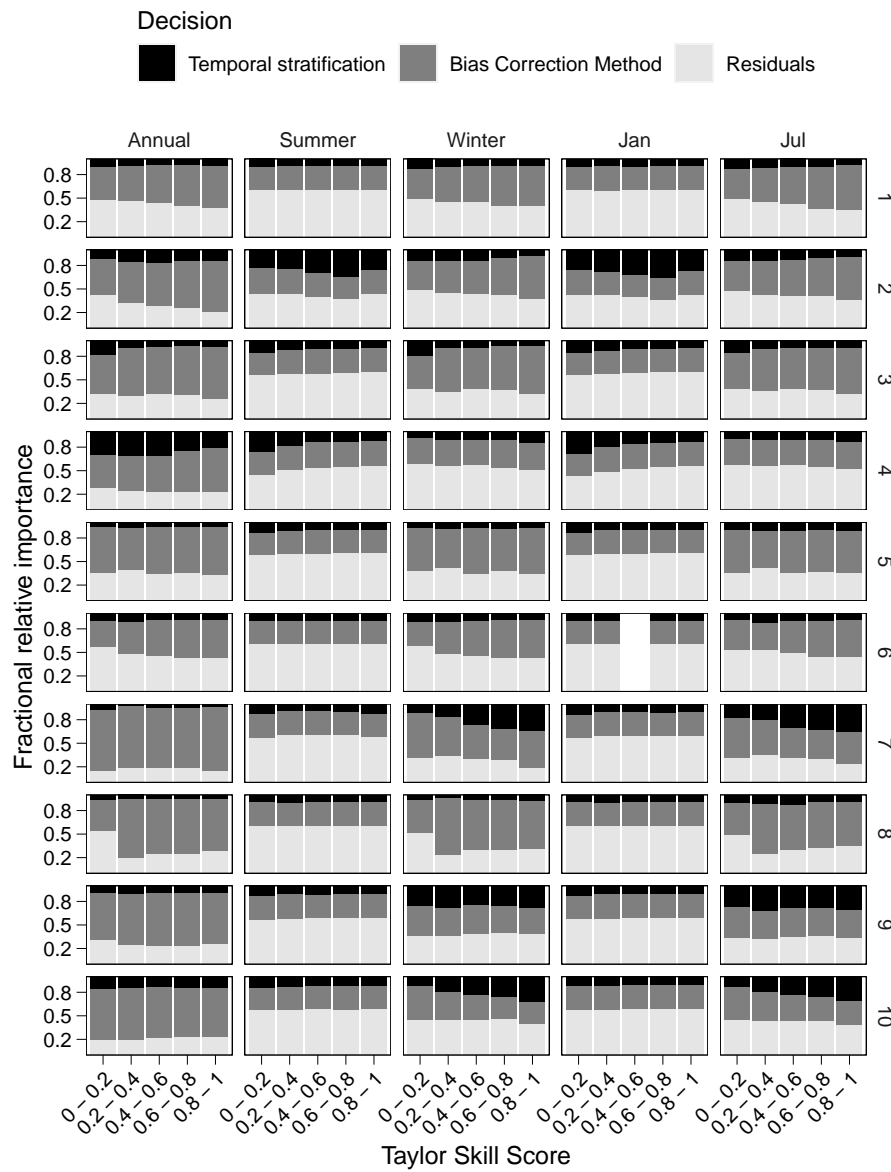


Figure S19. Same as in Figure S11, but for the snowfall fraction.